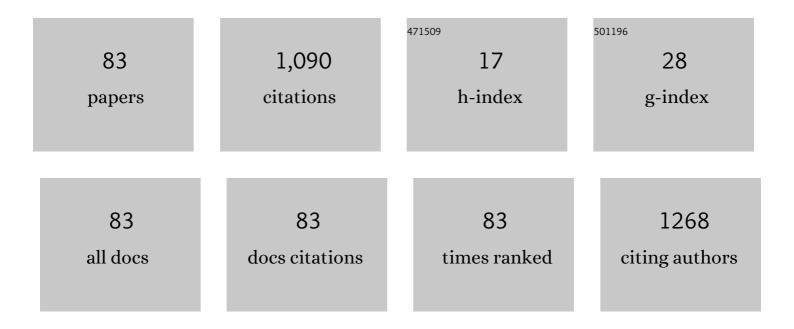
## Tomasz Tokarski

List of Publications by Year in descending order

Source: https://exaly.com/author-pdf/351190/publications.pdf Version: 2024-02-01



#	Article	IF	CITATIONS
1	Improvement of TiC/Fe in situ composite layer formation on surface of Fe-based castings. Materials Letters, 2022, 309, 131399.	2.6	3
2	Microstructure Evolution in Inconel 718 Produced by Powder Bed Fusion Additive Manufacturing. Journal of Manufacturing and Materials Processing, 2022, 6, 20.	2.2	3
3	Dry sliding, slurry abrasion and cavitation erosion of composite layers reinforced by TiC fabricated in situ in cast steel and gray cast iron. Journal of Materials Processing Technology, 2022, 308, 117688.	6.3	8
4	Tetragonality mapping of martensite in a high‑carbon steel by EBSD. Materials Characterization, 2021, 175, 111040.	4.4	13
5	Crystallographic analysis of the lattice metric ( <i>CALM</i> ) from single electron backscatter diffraction or transmission Kikuchi diffraction patterns. Journal of Applied Crystallography, 2021, 54, 1012-1022.	4.5	10
6	Kikuchi pattern simulations of backscattered and transmitted electrons. Journal of Microscopy, 2021, 284, 157-184.	1.8	10
7	Transmission Kikuchi diffraction: The impact of the signal-to-noise ratio. Ultramicroscopy, 2021, 230, 113372.	1.9	5
8	Batch Reactor vs. Microreactor System for Efficient AuNP Deposition on Activated Carbon Fibers. Materials, 2021, 14, 6598.	2.9	1
9	Correlative Analysis of the Dimensional Properties of Bipyramidal Titania Nanoparticles by Complementing Electron Microscopy with Other Methods. Nanomaterials, 2021, 11, 3359.	4.1	6
10	Failure of the tail rotor of the Mi-24 helicopter as a result of a long-term impact of spatial resonance coupling. Journal of KONBiN, 2021, 51, 11-24.	0.4	2
11	Eco Friendly Synthesis of Carbon Dot by Hydrothermal Method for Metal Ions Salt Identification. Materials, 2021, 14, 7604.	2.9	17
12	2H and 4H silver colloidal suspension synthesis, as a new potential drug carrier. Chemical Engineering Journal, 2020, 382, 122922.	12.7	6
13	Refined Calibration Model for Improving the Orientation Precision of Electron Backscatter Diffraction Maps. Materials, 2020, 13, 2816.	2.9	17
14	Approximant-based orientation determination of quasicrystals using electron backscatter diffraction. Ultramicroscopy, 2020, 218, 113093.	1.9	5
15	Strain Localization During Compressive Deformation of Mg-Gd Alloy. Metallurgical and Materials Transactions A: Physical Metallurgy and Materials Science, 2020, 51, 3742-3748.	2.2	8
16	EBSD orientation analysis based on experimental Kikuchi reference patterns. Acta Materialia, 2020, 188, 376-385.	7.9	29
17	Manual measurement of angles in backscattered and transmission Kikuchi diffraction patterns. Journal of Applied Crystallography, 2020, 53, 435-443.	4.5	3
18	Temperature dependence of twinning stress in Ni49.5Mn38.4Sn12.2 single crystal. Journal of Applied Physics 2019 126 145107	2.5	2

#	Article	IF	CITATIONS
19	Monitoring wear of gear wheel of helicopter transmission using the FAM-C and FDM-A methods. Procedia Structural Integrity, 2019, 16, 184-191.	0.8	6
20	The Effect of Fe Addition on Fragmentation Phenomena, Macrostructure, Microstructure, and Hardness of TiC-Fe Local Reinforcements Fabricated In Situ in Steel Casting. Metallurgical and Materials Transactions A: Physical Metallurgy and Materials Science, 2019, 50, 975-986.	2.2	14
21	Local composite reinforcements of TiC/FeMn type obtained in situ in steel castings. Archives of Civil and Mechanical Engineering, 2019, 19, 997-1005.	3.8	14
22	2019, 171, 107703.	7.0	37
23	Continuous, monodisperse silver nanoparticles synthesis using microdroplets as a reactor. Journal of Flow Chemistry, 2019, 9, 1-7.	1.9	22
24	High-spatial resolution dating of monazite and zircon revealsÂthe timing of subduction–exhumation of the Vaimok Lens in the Seve Nappe Complex (Scandinavian Caledonides). Contributions To Mineralogy and Petrology, 2019, 174, 1.	3.1	36
25	Orthogonal shear process in Ni-Mn-Sn single crystal. International Journal of Plasticity, 2019, 114, 63-71.	8.8	14
26	Superelastic behavior of a metamagnetic Ni–Mn–Sn single crystal. Journal of Materials Science, 2018, 53, 10383-10395.	3.7	14
27	Palladium(II) Chloride Complex Ion Recovery from Aqueous Solutions Using Adsorption on Activated Carbon. Journal of Chemical & Engineering Data, 2018, 63, 702-711.	1.9	45
28	TiC – Based local composite reinforcement obtained in situ in ductile iron based castings with use of rode preform. Materials Letters, 2018, 222, 192-195.	2.6	15
29	Deposition of Pd nanoparticles on the walls of cathodically hydrogenated TiO2 nanotube arrays via galvanic displacement: A novel route to produce exceptionally active and durable composite electrocatalysts for cost-effective hydrogen evolution. Nano Energy, 2018, 47, 527-538.	16.0	32
30	Strain-induced martensite reversion in 18Cr–8Ni steel – transmission Kikuchi diffraction study. Materials Science and Technology, 2018, 34, 580-583.	1.6	5
31	Novel and effective synthesis protocol of AgNPs functionalized using L-cysteine as a potential drug carrier. Naunyn-Schmiedeberg's Archives of Pharmacology, 2018, 391, 123-130.	3.0	19
32	Ni-Cr-Ta-Al-C complex phase alloy – Design, microstructure and properties. Materials Science & Engineering A: Structural Materials: Properties, Microstructure and Processing, 2018, 711, 99-108.	5.6	2
33	Martensite stabilisation in single crystalline Ni-Mn-Ga and Ni-Mn-Sn magnetic shape memory alloys. Materials Letters, 2018, 230, 266-269.	2.6	13
34	Reactive casting coatings for obtaining in situ composite layers based on Fe alloys. Surface and Coatings Technology, 2018, 350, 346-358.	4.8	8
35	Mapping of local lattice parameter ratios by projective Kikuchi pattern matching. Physical Review Materials, 2018, 2, .	2.4	15
36	The effect of temperature on the evolution of eutectic carbides and M 7 C 3 Â→ÂM 23 C 6 carbides reaction in the rapidly solidified Fe-Cr-C alloy. Journal of Alloys and Compounds, 2017, 698, 673-684.	5.5	104

Tomasz Tokarski

#	Article	IF	CITATIONS
37	Branched needle microstructure in Ni-Mn-Ga 10M martensite: EBSD study. Acta Materialia, 2017, 128, 113-119.	7.9	14
38	Wear Resistance of TiC Reinforced Cast Steel Matrix Composite. Archives of Foundry Engineering, 2017, 17, 143-146.	0.4	4
39	The γ′-Ni 3 (Al,Ta) phase triggered strengthening of the Ni-Ta-Al-Cr-C coating layer, deposited on austenitic stainless steel. Materials Characterization, 2017, 129, 367-377.	4.4	10
40	Micromechanical behaviour of a two-phase Ti alloy studied using grazing incidence diffraction and a self-consistent model. Acta Materialia, 2017, 136, 402-414.	7.9	9
41	The Investigation of Strain-Induced Martensite Reverse Transformation in AISI 304 Austenitic Stainless Steel. Metallurgical and Materials Transactions A: Physical Metallurgy and Materials Science, 2017, 48, 4999-5008.	2.2	52
42	Experimental study of phase transformation in non-equilibrium hypoeutectic alloy from the Fe–Cr–Ni–Mo–C system. Journal of Thermal Analysis and Calorimetry, 2017, 127, 449-455.	3.6	4
43	The Analysis of Foundry Engineering of Copper Alloys Based on the Research of a Metallurgist Settlement in SzczepidÅ,o. Archives of Foundry Engineering, 2017, 17, 45-50.	0.4	4
44	The Analysis of the Water-Expanded Rock Bolts Ruptures During Pressure Test. Archives of Mining Sciences, 2017, 62, 423-430.	0.6	1
45	Mechanical Properties of Solid-State Recycled 4xxx Aluminum Alloy Chips. Journal of Materials Engineering and Performance, 2016, 25, 3252-3259.	2.5	13
46	Locally Reinforcement TiC-Fe Type Produced in Situ in Castings. Archives of Foundry Engineering, 2016, 16, 77-82.	0.4	3
47	Experimental and Thermodynamic Study of Selected in-Situ Composites from the Fe-Cr-Ni-Mo-C System. Archives of Metallurgy and Materials, 2016, 61, 1241-1247.	0.6	3
48	Computer Simulation of the Formation of Non-Metallic Precipitates During a Continuous Casting of Steel. Archives of Metallurgy and Materials, 2016, 61, 335-340.	0.6	0
49	Hardness and Wear Resistance of TiC-Fe-Cr Locally Reinforcement Produced in Cast Steel. Archives of Foundry Engineering, 2016, 16, 89-94.	0.4	8
50	Comparative Analysis of Properties and Microstructure of the Plastically Deformed Alloy Inconel®718, Manufactured by Plastic Working and Direct Metal Laser Sintering. Archives of Metallurgy and Materials, 2016, 61, 143-148.	0.6	8
51	High quality transmission Kikuchi diffraction analysis of deformed alloys - Case study. Materials Characterization, 2016, 121, 231-236.	4.4	15
52	Crystallography and Morphology of Chromium Rich Eutectic Carbides in an As-Cast Fe-Cr-C Alloy Crystallized in Non-Equilibrium Conditions. Acta Physica Polonica A, 2016, 130, 1007-1009.	0.5	4
53	X-ray Diffraction and EBSD Study of Al-Ti-Co-Ni-Fe High-Entropy Alloy. Acta Physica Polonica A, 2016, 130, 991-992.	0.5	2
54	Microstructural Characteristic of Hypereutectoid Iron Alloys Melted in ArcMelter Furnace. Acta Physica Polonica A, 2016, 130, 939-941.	0.5	0

TOMASZ TOKARSKI

#	Article	IF	CITATIONS
55	Thermo-Mechanical Processing of Rapidly Solidified 5083 Aluminium Alloy - Structure and Mechanical Properties. Archives of Metallurgy and Materials, 2015, 60, 177-180.	0.6	6
56	Electrowinning Of Tellurium From Acidic Solutions. Archives of Metallurgy and Materials, 2015, 60, 591-596.	0.6	13
57	Effect Of Heat Treatment On The Corrosion Resistance Of Aluminized Steel Strips. Archives of Metallurgy and Materials, 2015, 60, 1825-1832.	0.6	6
58	Photoelectrochemistry of n-type antimony sulfoiodide nanowires. Nanotechnology, 2015, 26, 105710.	2.6	28
59	Effect of SPS parameters on densification and properties of steel matrix composites. Advanced Powder Technology, 2015, 26, 1152-1161.	4.1	43
60	Microstructure and texture characteristics of the metastable Fe–21Mn–3Si–3Al alloy after cold deformation. Journal of Alloys and Compounds, 2015, 643, S39-S45.	5.5	14
61	Lead molybdate – a promising material for optoelectronics and photocatalysis. Journal of Materials Chemistry C, 2015, 3, 2614-2623.	5.5	26
62	Cast aluminium matrix composites modified with using FSP process – Changing of the structure and mechanical properties. Composite Structures, 2015, 133, 959-967.	5.8	42
63	Magnetic field effect on the electrodeposition of ZnSe. Magnetohydrodynamics, 2015, 51, 345-352.	0.3	5
64	Effect of Compaction Pressure Applied to TiC Reactants on the Microstructure and Properties of Composite Zones Produced <i>In Situ</i> in Steel Castings. Materials Science Forum, 2014, 782, 527-532.	0.3	7
65	Electrodeposition of Co–Pd alloys from ammonia solutions and their catalytic activity for hydrogen evolution reaction. Journal of Applied Electrochemistry, 2014, 44, 97-103.	2.9	35
66	Bi <sub>x</sub> La <sub>1â^'x</sub> VO <sub>4</sub> solid solutions: tuning of electronic properties via stoichiometry modifications. Nanoscale, 2014, 6, 2244-2254.	5.6	22
67	Sintered Fe-Ni-Cu-Sn-C Alloys Made of Ball-Milled Powders. Archives of Metallurgy and Materials, 2014, 59, 947-950.	0.6	6
68	The Use of Colloidal Solutions of Zinc Oxide Nanoparticles in Investment Casting Technology/ Wykorzystanie Koloidalnych Roztworów Nanoczastek Tlenku Cynku W Technologii Wytapianych Modeli. Archives of Metallurgy and Materials, 2014, 59, 1355-1359.	0.6	0
69	High-cycle fatigue bending strength of rapidly solidified and plastic consolidated RS442 aluminium alloy. Journal of Materials Science, 2013, 48, 4796-4800.	3.7	2
70	Novel, Microwave Assisted Route of Synthesis of Binary Oxide Semiconducting Phases – PbMoO4 And PbWo4 / Nowa Metoda Syntezy Binarnych Faz Tlenkowych O Charakterze PóÅ,przewodnikowym W Polu Mikrofalowym – PbMoO4 I PbWo4. Archives of Metallurgy and Materials, 2013, 58, 217-222.	0.6	18
71	Kinetic Study of The Photoelectrochemical Gold Recovery from Diluted Chloride Solutions. Archives of Metallurgy and Materials, 2013, 58, 709-716.	0.6	7
72	Synthesis of Zno Nanoparticles by Thermal Decomposition of Basic Zinc Carbonate. Archives of Metallurgy and Materials, 2013, 58, 489-491.	0.6	21

Tomasz Tokarski

#	Article	IF	CITATIONS
73	Premature Cracking of Dies for Aluminium Alloy Die-Casting. Archives of Metallurgy and Materials, 2013, 58, 1275-1279.	0.6	2
74	The Effect of Reciprocating Extrusion (Cec) on the Consolidated Silver Powders Microstructure / WpÅ,yw Dwustronnego Wyciskania (Cws) Na Mikrostrukture Konsolidowanych Proszków Srebra. Archives of Metallurgy and Materials, 2013, 58, 73-75.	0.6	4
75	Composite Zones Produced in Iron Castings by In-Situ Synthesis of Tic Carbides. Archives of Metallurgy and Materials, 2013, 58, 465-471.	0.6	7
76	Composite Zones Obtained by in situ Synthesis in Steel Castings. Archives of Metallurgy and Materials, 2013, 58, 769-773.	0.6	9
77	Microstructure and Plasticity of Hot Deformed 5083 Aluminum Alloy Produced by Rapid Solidification and Hot Extrusion / Badania Mikrostruktury I PlastycznoÅ›ci OdksztaÅ,canego Na GorÄco Szybko-Krystalizowanego I Wyciskanego Stopu Aluminium 5083. Archives of Metallurgy and Materials, 2012. 57. 1253-1259.	0.6	9
78	The Effect of Plastic Consolidation Parameters on the Microstructure and Mechanical Properties of Various Aluminium Powders. Materials Science Forum, 2011, 674, 141-146.	0.3	1
79	Characterization of AM60 Magnesium Alloy Prepared by Rapid Solidification and Plastic Consolidation Technique. Materials Science Forum, 2010, 667-669, 997-1002.	0.3	0
80	Is there a critical resolved shear stress for twinning in face-centred cubic crystals?. Philosophical Magazine, 2004, 84, 481-502.	1.6	30
81	Effect of Rapid Solidification on the Structure and Mechanical Properties of AZ91 Magnesium Alloy. Solid State Phenomena, 0, 186, 120-123.	0.3	3
82	The Effect of Heat Treatment on Static and Dynamic Mechanical Properties of Rapidly Solidified and Plastically Consolidated RS442 Aluminium Alloy. Key Engineering Materials, 0, 641, 17-23.	0.4	0
83	Light Metals Chips Recycling by Plastic Consolidation. Key Engineering Materials, 0, 641, 24-29.	0.4	7